

Supplementary Information

The Role of Phosphorus in the Solid Electrolyte Interphase of Argyrodite Solid Electrolytes

Matthew Burton^{1,2}, Ben Jagger¹, Yi Liang¹, Joshua S. Gibson¹, Jack Aspinall¹, Zhongdui Long^{1,2}, Jack E. N. Swallow¹, Robert S. Weatherup^{1,3}, and Mauro Pasta^{1,2*}

¹Department of Materials, University of Oxford, Parks Road, Oxford OX1 3PH, United Kingdom

²The Faraday Institution, Quad One, Harwell Science and Innovation Campus, Didcot OX11 0RA, United Kingdom

³Diamond Light Source, Harwell Science and Innovation Campus, Didcot OX11 0DE, United Kingdom

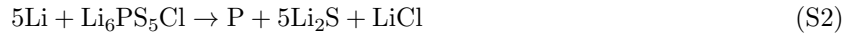
*Corresponding author: mauro.pasta@materials.ox.ac.uk

Supplementary Note 1: Stoichiometric Equations for the Chemical Reduction of Li₆PS₅Cl

The complete chemical reduction of Li₆PS₅Cl and all SEI components requires 8 Li atoms, as shown in Equation S1.



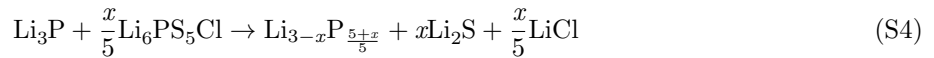
Thermodynamically, Li₆PS₅Cl could be chemically reduced with just 5 Li atoms,[1] as shown in Equation S2.



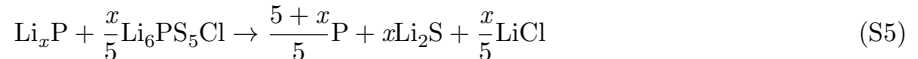
Thermodynamically, Li₆PS₅Cl could also be chemically reduced by Li₃P, as shown in Equation S3.



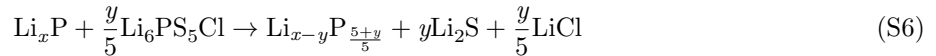
Additionally, Li₆PS₅Cl could also be chemically reduced by Li₃P resulting in a partially reduced P species existing, as shown in Equation S4.



Thermodynamically, Li₆PS₅Cl could also be chemically reduced by Li_xP (where x < 3), as shown in Equation S5.



Additionally, Li₆PS₅Cl could also be chemically reduced by Li_xP resulting in a partially reduced P species still existing, as shown in Equation S6, where y < x.



Supplementary Note 2: CTTA fitting to the Deal-Grove model

In the Deal-Grove model[2] film thickness, x_0 , is predicted to increase over time, t , according to:

$$x_0^2 + Ax_0 = B(t + \tau) \quad (S7)$$

where A and B are fitting constants and τ is a time offset allowing for an initial thickness at time $t = 0$.

In the long time limit, when $t \gg \frac{A^2}{4B}$, film growth is diffusion limited and Eq. S7 reduces to:

$$x_0 \approx \sqrt{Bt} \quad (S8)$$

Fitting CTTA data from Figure 1b gives a gradient which is equal to $B^{0.5}$. The gradient equals 1.423, which therefore give a B value of 2.025. Fitting the CTTA from Figure 1b to the Deal-Grove model, but fixing B as a value of 2.025 gives a negative A (-12.724) and τ (-19.988) (Figure S18) which is not physical. This indicates that the fit is not appropriate.

In the short time limit, when $t \ll \frac{A^2}{4B}$, film growth is limited by reaction kinetics and Eq. S7 reduces to:

$$x_0 \approx \frac{B}{A}(t + \tau) \quad (S9)$$

Fitting the first two CTTA data points as linear gives a gradient and thus B/A of 1.567, thus using the previously deduced B gives an A of 1.292. Taking this A and B would define short time as $\ll 0.21$ h. The first plating step in the CTTA alone is 0.1 h, therefore, this would imply the kinetically limited regime is not accessible in the time frame of the CTTA experiment.

Supplementary Note 3: Transmission Line Model Fitting of the SEI

The SEI is modeled as a long open uniform distributed transmission line, which can be approximated as a M_a element.[3] The relationship between the impedance from a M_a element and the resistance of the SEI (R_{SEI}) is shown in Equation S10.

$$Z_{M_a} = R_{SEI} \frac{\coth((\tau j\omega)^{\alpha/2})}{(\tau j\omega)^{\alpha/2}} \quad (S10)$$

Additional data

Supplementary Table 1 Volume fractions of the SEI of $\text{Li}_6\text{PS}_5\text{Cl}$ if P is fully lithiated

Species	Molar Volume ($\text{cm}^3 \text{ mol}^{-1}$)	Molar Ratio	Product ($\text{cm}^3 \text{ mol}^{-1}$)	Volume Fraction (%)
Li_2S	27.5	5	137.5	70.8
LiCl	20.5	1	20.5	10.6
Li_3P	36.2	1	36.2	18.6
Total			194.2	

Supplementary Table 2 Volume fractions of the SEI of $\text{Li}_{5.7}\text{PS}_{4.7}\text{Cl}_{0.65}\text{Br}_{0.65}$ if P is fully lithiated

Species	Molar Volume ($\text{cm}^3 \text{ mol}^{-1}$)	Molar Ratio	Product ($\text{cm}^3 \text{ mol}^{-1}$)	Volume Fraction (%)
Li_2S	27.5	4.7	129.3	66.3
LiCl	20.5	0.65	13.3	6.8
LiCl	20.5	0.65	16.3	8.4
Li_3P	36.2	1	36.2	18.6
Total			195.1	

Supplementary Table 3 Volume fractions of the SEI of $\text{Li}_{5.5}\text{PS}_{4.5}\text{Cl}_{0.75}\text{Br}_{0.75}$ if P is fully lithiated

Species	Molar Volume ($\text{cm}^3 \text{ mol}^{-1}$)	Molar Ratio	Product ($\text{cm}^3 \text{ mol}^{-1}$)	Volume Fraction (%)
Li_2S	27.5	4.5	123.8	63.7
LiCl	20.5	0.75	15.4	7.9
LiCl	20.5	0.75	18.8	9.7
Li_3P	36.2	1	36.2	18.6
Total			194.2	

Supplementary Table 4 Volume fractions of the SEI of Li₆PS₅Cl if P is not lithiated

Species	Molar Volume (cm ³ mol ⁻¹)	Molar Ratio	Product (cm ³ mol ⁻¹)	Volume Fraction (%)
Li ₂ S	27.5	5	137.5	80.4
LiCl	20.5	1	20.5	12.0
P	13	1	13	7.6
Total			171.0	

Supplementary Table 5 Fitting parameters and fit quality data not otherwise plotted of the growing SEI PEIS

Accumulated Charge (μA h cm ⁻²)	t (s)	Q (nF s ^{α-1})	α	α2	χ ² Z ⁻¹
1.56	7.488E-5	24.06	0.9003	0.6323	0.00486
3.12	1.946E-4	18.5	0.9241	0.6535	0.00475
4.68	2.336E-4	34.23	0.8721	0.6585	0.00196
6.24	4.19E-4	25.98	0.8943	0.6684	0.00433
7.8	5.665E-4	50.27	0.8332	0.6771	0.00824
9.35	7.003E-4	16.88	0.9378	0.6741	0.00268
10.9	9.8E-4	14.22	0.9536	0.6843	0.00805
12.5	0.00119	22.8	0.9118	0.6913	0.01348
14	0.00138	15.64	0.9503	0.6922	0.01118
15.6	0.0013	19.64	0.9348	0.6832	0.00487
17.1	0.00159	19.37	0.9384	0.69	0.00868
18.7	0.00199	18.23	0.9445	0.6989	0.01536
20.3	0.00216	19.09	0.9387	0.6988	0.01563
21.8	0.00252	18.72	0.943	0.7037	0.02281
23.4	0.0023	22.7	0.9291	0.6933	0.01358
24.9	0.00251	24.41	0.928	0.6937	0.0168
26.5	0.00272	16.11	0.9636	0.693	0.00903
28.1	0.00269	27.36	0.9205	0.6897	0.0159
29.6	0.00262	20.99	0.9502	0.6811	0.01031
31.2	0.00286	33.48	0.9142	0.6853	0.01764
32.7	0.00281	23.62	0.9438	0.6775	0.01066
34.3	0.00312	26.36	0.9421	0.6811	0.01668
35.9	0.0034	43.29	0.901	0.6836	0.02181
37.4	0.00349	47.66	0.8952	0.6808	0.0238
39	0.00364	50.1	0.8945	0.6789	0.00679
40.5	0.00379	30.99	0.9361	0.6738	0.02111
42.1	0.00405	62.51	0.8789	0.6789	0.03087
43.7	0.00377	46.45	0.9074	0.6682	0.04869
45.2	0.00414	47.61	0.9067	0.6706	0.02442
46.8	0.00377	86.67	0.8564	0.6635	0.02239
48.3	0.00432	52.86	0.9003	0.6679	0.024
49.9	0.00402	61.59	0.8888	0.6604	0.01922

Supplementary Table 6 Fitting parameters and fit quality data not otherwise plotted of the OCV SEI PEIS

OCV time (h)	t (s)	Q (nF s ^{α-1})	α	α2	χ ² Z ⁻¹
0	0.00402	61.59	0.8888	0.6604	0.01922
25	0.00403	93.56	0.8574	0.6689	0.02222
50	0.00479	75.96	0.8751	0.6437	0.0061
75	0.00326	68.54	0.8831	0.6369	0.0052
100	0.00297	71.2	0.8789	0.6219	0.00898
125	0.004	63.82	0.8885	0.6539	0.00697
150	0.00368	67.29	0.885	0.6459	0.006
175	0.00375	71.57	0.8802	0.6497	0.00618
200	0.00348	74.68	0.8781	0.6469	0.0062
225	0.0036	71.4	0.8816	0.6512	0.00638
250	0.00318	66	0.8878	0.6392	0.0057
275	0.00328	64.64	0.8903	0.6483	0.00668
300	0.00297	47.76	0.9147	0.6437	0.01538
325	0.00306	51.86	0.9044	0.6481	0.01597
350	0.00312	37.1	0.9295	0.6468	0.01163
375	0.00295	40.76	0.9223	0.6469	0.01273
400	0.00288	52.44	0.9048	0.6611	0.02028

Supplementary Table 7 XPS fitting parameters after VEP on a $\text{Li}_6\text{PS}_5\text{Cl}$ pellet, corresponding to Fig. 3a and Supplementary Fig. S6.

Transition	Species	Binding Energy (eV)	FWHM (eV)	Spin-Orbit Splitting (eV)
S 2p	$\text{Li}_6\text{PS}_5\text{Cl}$	161.4 ± 0.1	1.15 ± 0.08	1.2
	Li_2S	160.1 ± 0.1	1.13 ± 0.03	1.2
P 2p	$\text{Li}_6\text{PS}_5\text{Cl}$	132.0 ± 0.1	1.90 ± 0.01	0.9
	Li_xP	128.9 ± 0.1	1.7 ± 0.2	0.9
	Li_yP	127.2 ± 0.1	1.7 ± 0.2	0.9
	Li_3P	125.8	1.51	0.9

Supplementary Table 8 XPS fitting parameters during VEP on a phosphorus-coated $\text{Li}_6\text{PS}_5\text{Cl}$ pellet, corresponding to Fig. 4a.

Transition	Species	Binding Energy (eV)	FWHM (eV)	Spin-Orbit Splitting (eV)
S 2p	P–S–P	162.6	1.15	1.2
	$\text{Li}_6\text{PS}_5\text{Cl}$	161.4 ± 0.1	1.10 ± 0.02	1.2
	Li_2S	160.1 ± 0.1	1.10 ± 0.02	1.2
P 2p	P–O	133.1 ± 0.1	1.4 ± 0.2	0.9
	$\text{Li}_6\text{PS}_5\text{Cl}$	131.8 ± 0.1	1.4 ± 0.2	0.9
	P^0	129.1 ± 0.2	1.4 ± 0.2	0.9
	Li_xP	127.7 ± 0.1	1.4 ± 0.2	0.9
	Li_yP	126.9 ± 0.1	1.4 ± 0.2	0.9
	Li_3P	125.7 ± 0.1	1.5 ± 0.2	0.9

Supplementary Table 9 SOXPES and HAXPES fitting parameters from a pristine $\text{Li}_6\text{PS}_5\text{Cl}$ pellet, corresponding to Supplementary Fig. S10.

Transition	Species	Binding Energy (eV)	FWHM (eV)	Spin-Orbit Splitting (eV)
SOXPES				
O 1s	Li_2CO_3	531.6	1.43	–
	LiOH	530.7	1.43	–
Cl 2p	$\text{Li}_6\text{PS}_5\text{Cl}$	198.5	1.10	1.6
P 2s	$\text{Li}_6\text{PS}_5\text{Cl}$	189.4	1.18	–
S 2p	Li_2SO_4	166.7	0.81	1.2
	$\text{Li}_6\text{PS}_5\text{Cl}$	161.3	0.81	1.2
	Li_2S	160.0	0.81	1.2
P 2p	$\text{Li}_6\text{PS}_5\text{Cl}$	131.9	0.68	0.9
Li 1s	$\text{Li}_6\text{PS}_5\text{Cl}$	55.7	1.36	–
2.2 keV				
O 1s	Li_2CO_3	531.6	1.43	–
	LiOH	530.6	1.43	–
Cl 2p	$\text{Li}_6\text{PS}_5\text{Cl}$	198.5	1.11	1.6
P 2s	$\text{Li}_6\text{PS}_5\text{Cl}$	189.3	1.35	–
S 2p	Li_2SO_4	166.7	0.82	1.2
	$\text{Li}_6\text{PS}_5\text{Cl}$	161.2	0.82	1.2
	Li_2S	159.9	0.82	1.2
P 2p	$\text{Li}_6\text{PS}_5\text{Cl}$	131.5	0.70	0.9
Li 1s	$\text{Li}_6\text{PS}_5\text{Cl}$	55.2	1.42	–
6.6 keV				
O 1s	Li_2CO_3	531.7	1.38	–
	LiOH	530.7	1.38	–
Cl 2p	$\text{Li}_6\text{PS}_5\text{Cl}$	198.5	1.03	1.6
P 2s	$\text{Li}_6\text{PS}_5\text{Cl}$	189.4	1.41	–
S 2p	Li_2SO_4	166.6	0.81	1.2
	$\text{Li}_6\text{PS}_5\text{Cl}$	161.2	0.81	1.2
	Li_2S	159.9	0.81	1.2
P 2p	$\text{Li}_6\text{PS}_5\text{Cl}$	131.5	0.68	0.9
Li 1s	$\text{Li}_6\text{PS}_5\text{Cl}$	55.4	1.38	–

Supplementary Table 10 SOXPES and HAXPES fitting parameters after approximately 20 nm of Li was evaporated onto a Li₆PS₅Cl pellet (0 h / 6 h / 12 h), corresponding to Fig. 5a, 5c and Supplementary Fig. S11.

Transition	Species	Binding Energy (eV)	FWHM (eV)	Spin-Orbit Splitting (eV)
SOXPES				
O <i>1s</i>	Li ₂ CO ₃	531.8 / 531.6 / 531.6	1.40 / 1.63 / 1.59	–
	LiOH	530.7 / 530.6 / 530.7	1.40 / 1.63 / 1.59	–
	Oxide	529.1 / – / –	1.42 / – / –	–
	Li ₂ O	528.1 / 528.1 / 528.2	1.42 / 1.46 / 1.39	–
Cl <i>2p</i>	Li ₆ PS ₅ Cl/LiCl	198.5 / 198.5 / 198.5	1.14 / 1.12 / 1.12	1.6
S <i>2p</i>	Li ₂ SO ₄	166.5 / – / –	0.92 / – / –	1.2
	Li ₆ PS ₅ Cl	161.3 / 161.4 / 161.3	0.92 / 0.91 / 0.90	1.2
	Li ₂ S	160.0 / 160.1 / 160.0	0.92 / 0.91 / 0.90	1.2
Li <i>1s</i>	Li ⁺	53.4 / 53.8 / 53.9	1.75 / 1.83 / 1.78	–
	Li ⁰	52.2 / 52.2 / 52.2	0.35 / 0.35 / 0.34	–
2.2 keV				
O <i>1s</i>	Li ₂ CO ₃	531.7 / 531.6 / 531.8	1.88 / 1.64 / 1.61	–
	LiOH	530.6 / 530.7 / 530.7	1.88 / 1.64 / 1.61	–
	Li ₂ O	528.2 / 528.2 / 528.2	1.34 / 1.24 / 1.21	–
Cl <i>2p</i>	Li ₆ PS ₅ Cl/LiCl	198.5 / 198.5 / 198.5	1.14 / 1.10 / 1.09	1.6
S <i>2p</i>	Li ₆ PS ₅ Cl	161.2 / 161.2 / 161.2	0.87 / 0.88 / 0.88	1.2
	Li ₂ S	160.0 / 160.0 / 160.0	0.87 / 0.88 / 0.88	1.2
P <i>2p</i>	Li ₆ PS ₅ Cl	131.6 / 131.6 / 131.5	0.73 / 0.78 / 0.90	0.9
	Li ₂ P	129.7 / 129.6 / 129.1	0.73 / 0.78 / 0.90	0.9
	Li ₄ P	128.0 / 127.8 / 127.2	0.73 / 0.78 / 0.90	0.9
	Li ₃ P	126.1 / 125.7 / 125.5	0.73 / 0.78 / 0.90	0.9
Li <i>1s</i>	Li ⁺	53.7 / 53.8 / 53.8	1.40 / 1.54 / 1.61	–
	Li ⁰	52.1 / 52.1 / 52.1	0.46 / 0.47 / 0.45	–
6.6 keV				
O <i>1s</i>	Li ₂ CO ₃	531.8 / 531.6 / 531.6	1.48 / 1.51 / 1.45	–
	LiOH	530.7 / 530.6 / 530.6	1.48 / 1.51 / 1.45	–
	Li ₂ O	528.2 / 528.1 / 528.1	1.31 / 1.23 / 1.22	–
Cl <i>2p</i>	Li ₆ PS ₅ Cl/LiCl	198.5 / 198.5 / 198.5	1.04 / 1.07 / 1.14	1.6
P <i>2s</i>	Li ₆ PS ₅ Cl	189.4 / 189.4 / 189.4	1.53 / 1.55 / 1.72	–
	Li ₂ P	187.3 / 187.2 / 186.9	1.53 / 1.55 / 1.72	–
	Li ₄ P	186.0 / 186.0 / 185.6	1.53 / 1.55 / 1.72	–
	Li ₃ P	184.2 / 183.9 / 183.7	1.53 / 1.55 / 1.72	–
S <i>2p</i>	Li ₆ PS ₅ Cl	161.2 / 161.2 / 161.2	0.85 / 0.86 / 0.86	1.2
	Li ₂ S	159.9 / 159.9 / 159.9	0.85 / 0.86 / 0.86	1.2
Li <i>1s</i>	Li ⁺	54.0 / 54.1 / 54.1	1.64 / 1.58 / 1.51	–
	Li ⁰	52.2 / 52.2 / 52.2	0.52 / 0.56 / 0.57	–

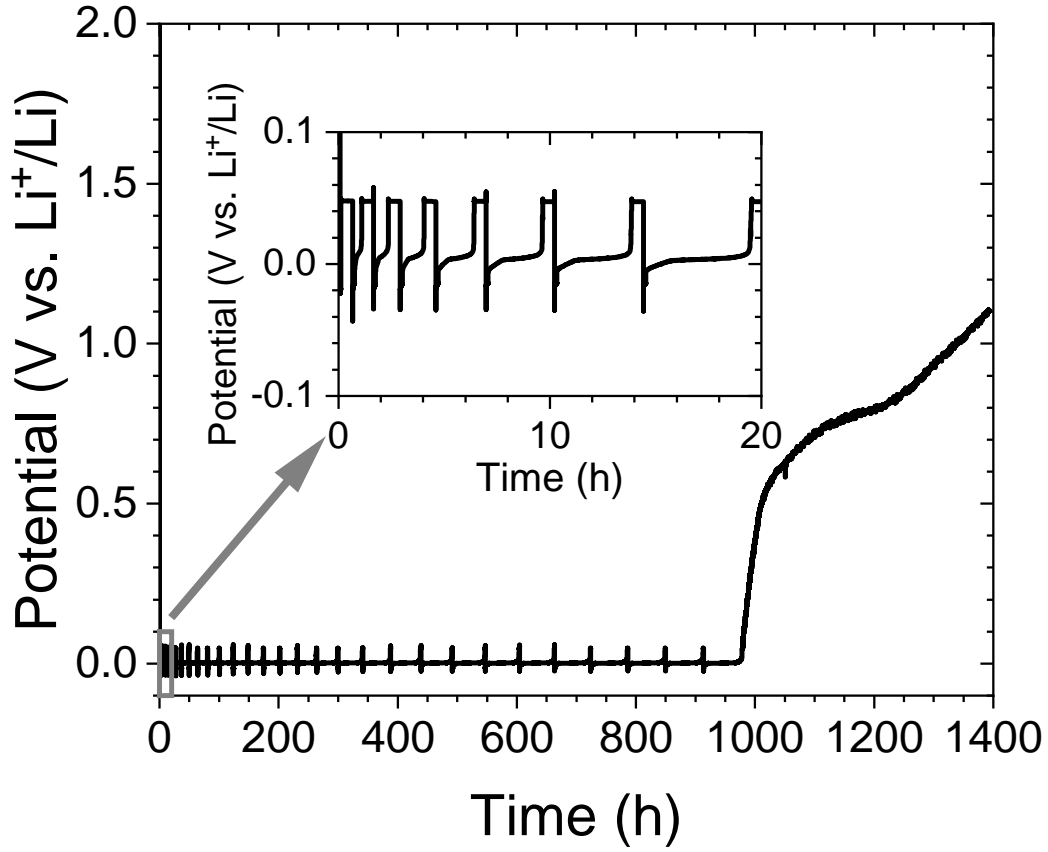


Figure S1: Three electrode CTTA measurement with PEIS conducted once a 50 mV OCV was reached (inset shows the initial cycles).

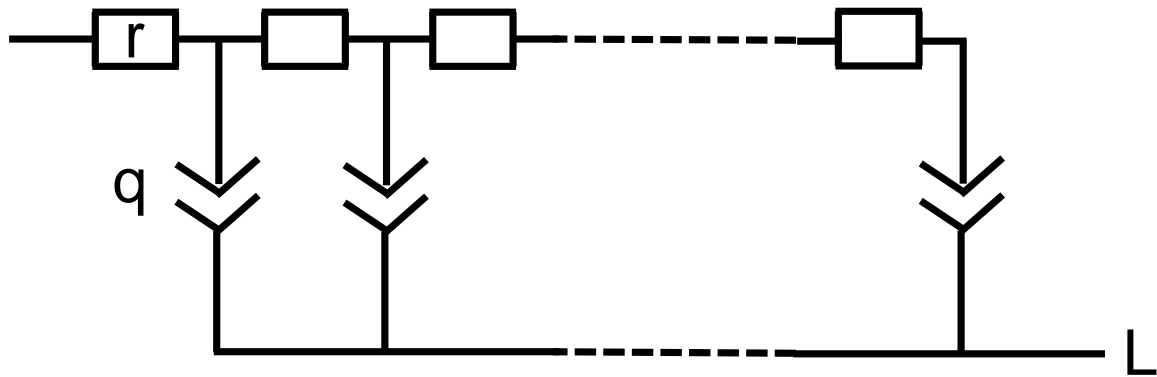


Figure S2: Equivalent circuit of the transmission line element; open-circuited uniform distributed resistor constant phase element (URQ), which is approximated as a M_a . [3] The resistance (R) of the transmission line is equal to the length (L) of the transmission line times by the resistivity (r) of the transmission line. This R is taken as the R_{SEI} in this work

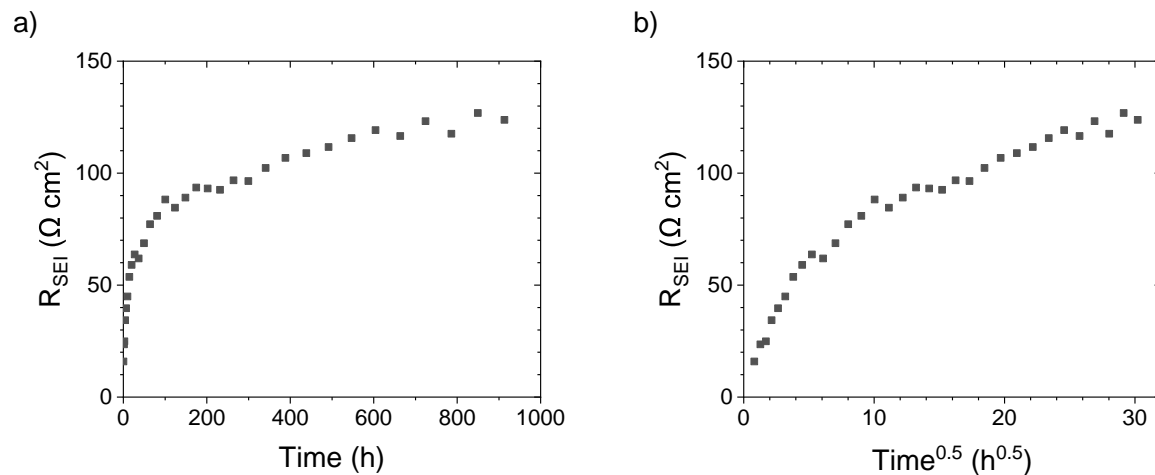


Figure S3: The increase in the SEI resistance against CTTA time, plotted with a) linear time and b) the square root of time. Source data are provided as a Source Data file.

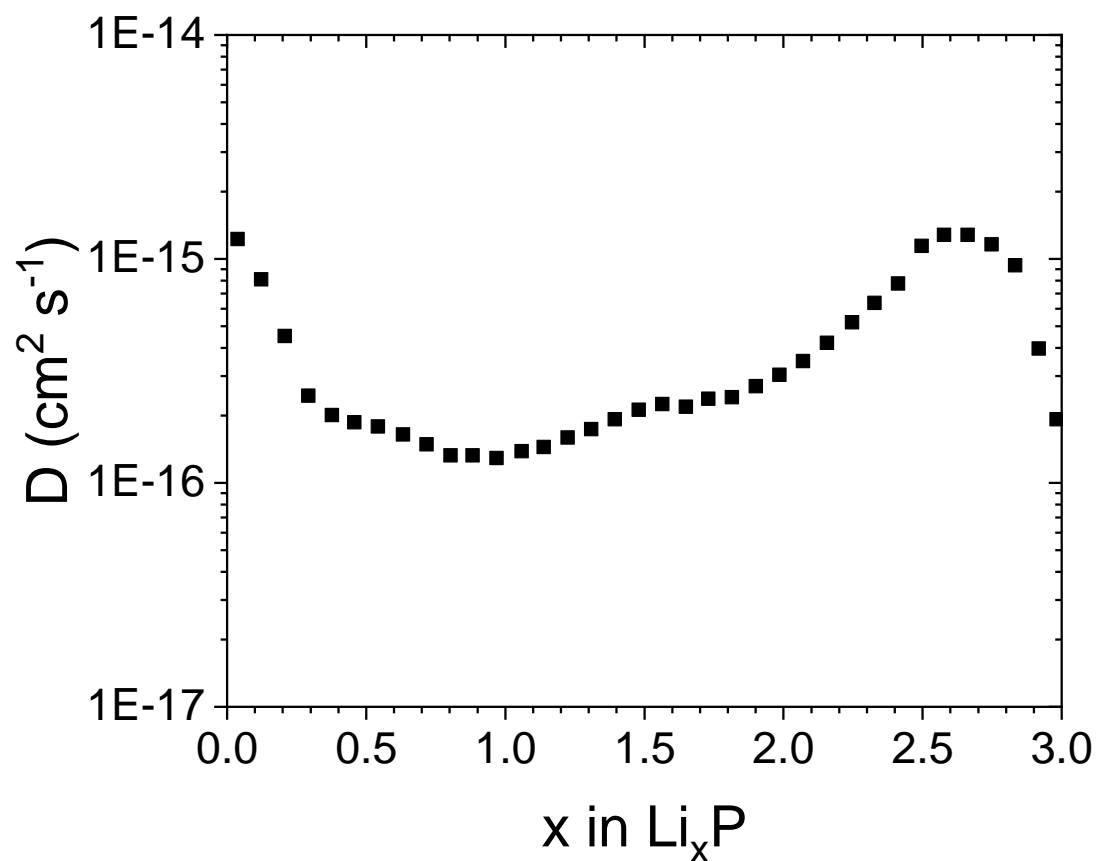


Figure S4: The suggested diffusivity of Li in Li_xP from GITT studies as reported by Capone *et al.*[4] Source data are provided as a Source Data file.

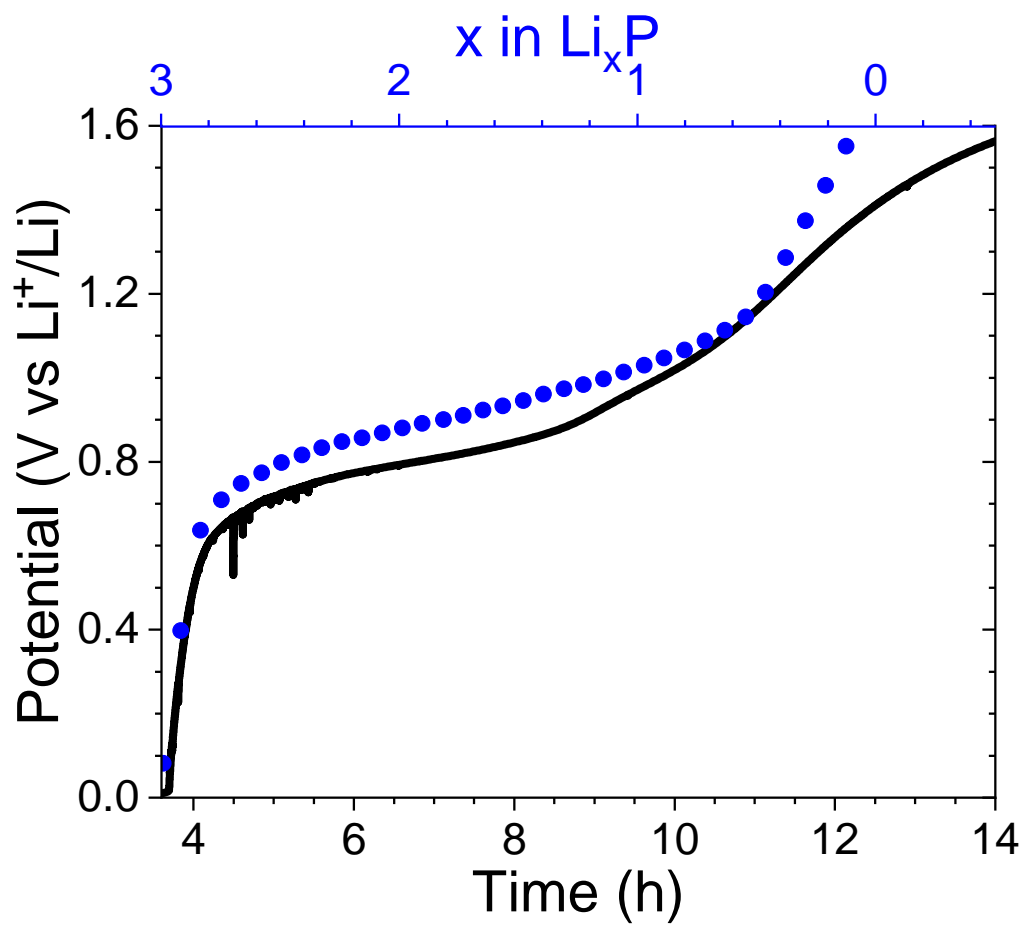


Figure S5: OCV times between 3.6 h and 14 h after 0.01 mAh of lithium was electroplated through a 1 cm diameter cylindrical pellet of $\text{Li}_6\text{PS}_5\text{Cl}$ over 1 hour (black line), compared to delithiation profile of red phosphorous from Capone *et al.* (blue circles).[4]

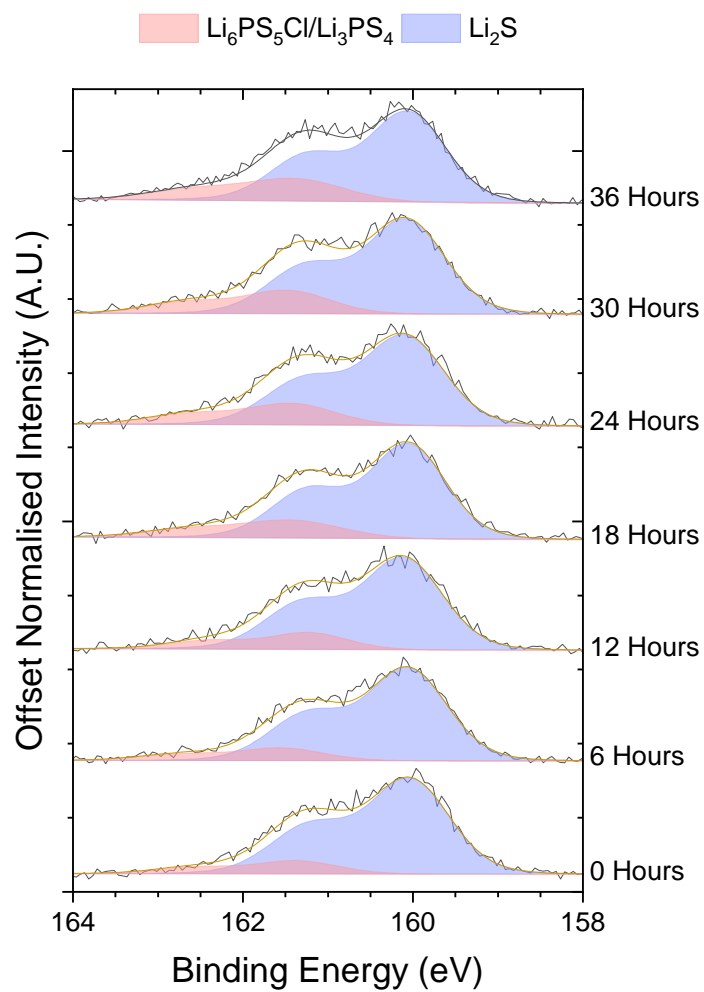


Figure S6: The sulphur $2p$ XPS data every 6 hours with the fitted components after $\sim 0.01 \text{ mAh cm}^{-2}$ of lithium was VEP through a $\text{Li}_6\text{PS}_5\text{Cl}$ pellet over 1 hour using an ebeam current of $2.5 \text{ }\mu\text{A}$ ($\sim 0.01 \text{ mA cm}^{-2}$). Source data are provided as a Source Data file.

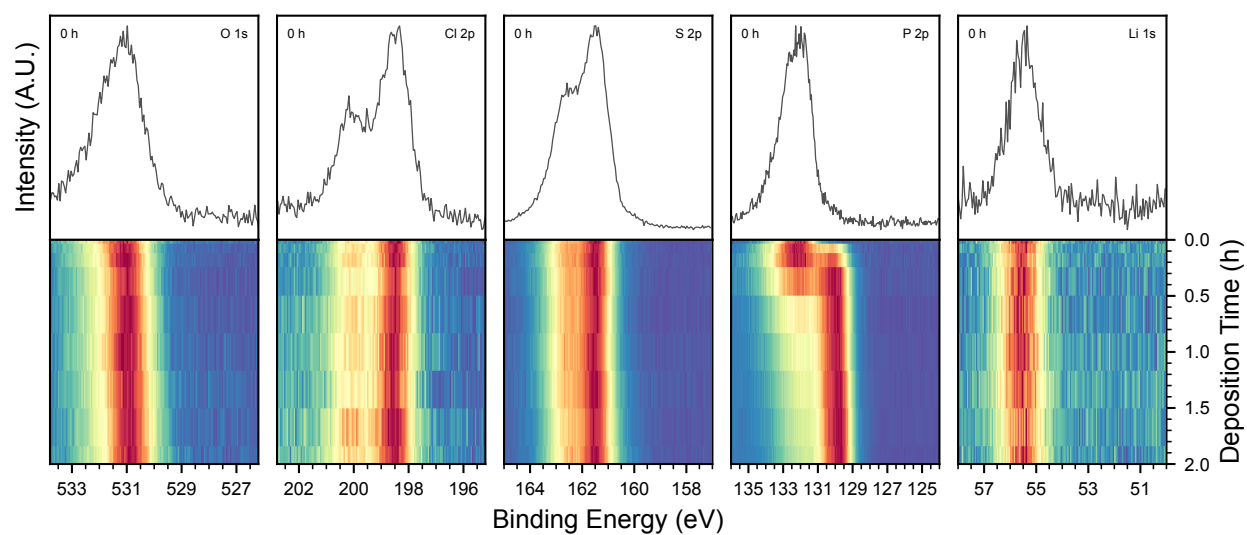


Figure S7: Normalised O *1s*, Cl *2p*, S *2p*, P *2p* and Li *1s* XPS spectra gathered during phosphorus sputtering onto a $\text{Li}_6\text{PS}_5\text{Cl}$ pellet for 2 h. Source data are provided as a Source Data file.

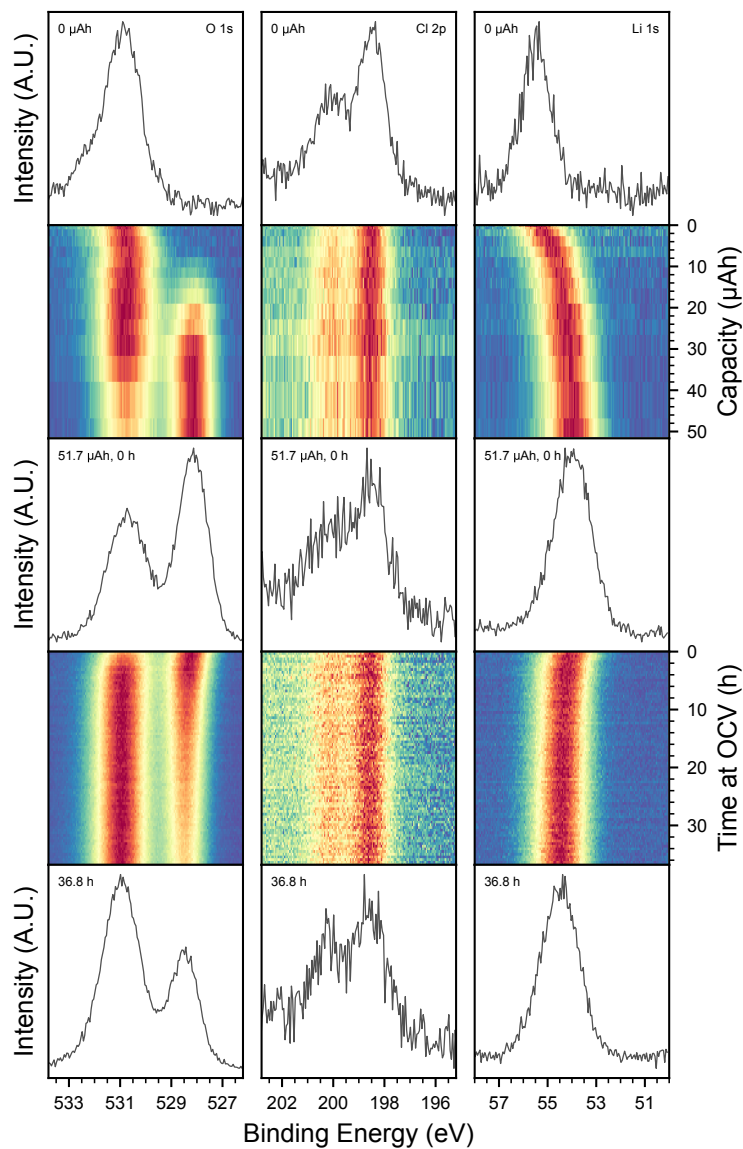


Figure S8: Evolution of the O 1s, Cl 2p and Li 1s spectra during VEP-XPS lithiation of a sputtered phosphorus layer on top of a $\text{Li}_6\text{PS}_5\text{Cl}$ pellet using an ebeam current of 30 μA to a capacity of 51.7 μAh ($\sim 0.26 \text{ mAh cm}^{-2}$), followed by resting under OCV for 36.8 h. All spectra have been normalised for clarity. Source data are provided as a Source Data file.

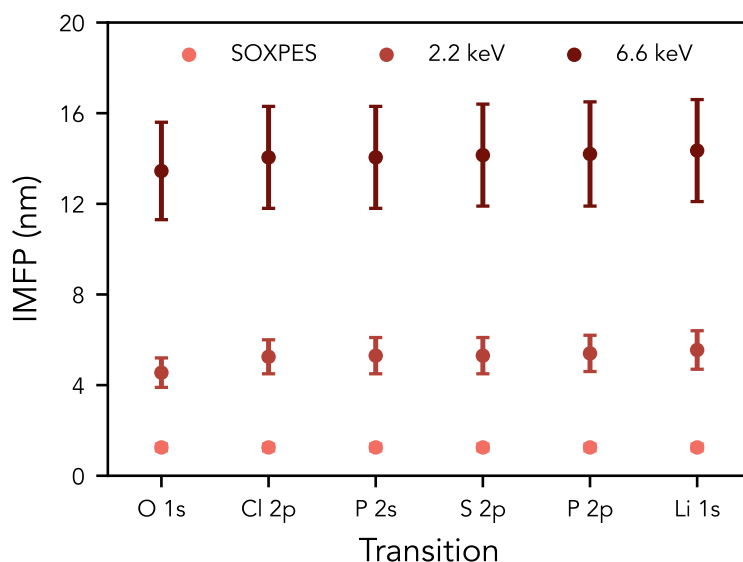


Figure S9: Electron inelastic-mean-free-paths (IMFPs) for each transition and incident photon energy calculated using the TPP-2M formula [5]. Upper and lower bounds are estimated by calculating the IMFP in Li^0 and $\text{Li}_6\text{PS}_5\text{Cl}$, respectively, whilst the center point represents the mean between these. Source data are provided as a Source Data file.

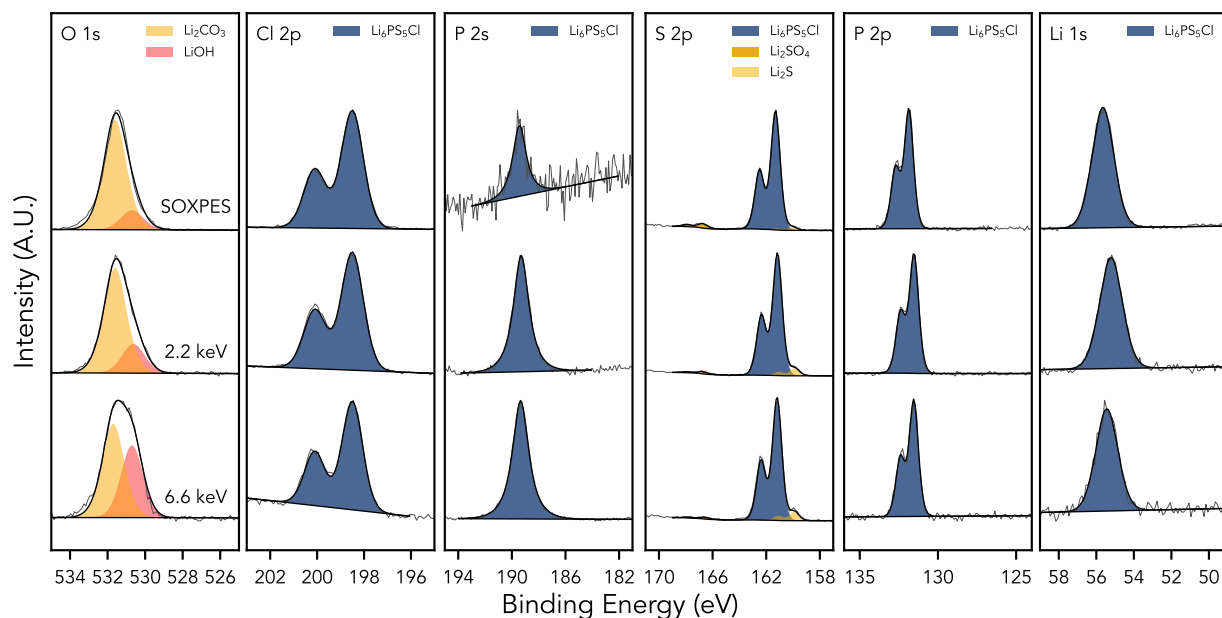


Figure S10: Full O 1s, Cl 2p, P 2s, S 2p, P 2p and Li 1s SOXPES and HAXPES spectra from a pristine $\text{Li}_6\text{PS}_5\text{Cl}$ pellet. Photoelectrons emitted during SOXPES have a kinetic energy of 315 eV, and HAXPES was performed with incident photon energies of 2.2 and 6.6 keV. Source data are provided as a Source Data file.

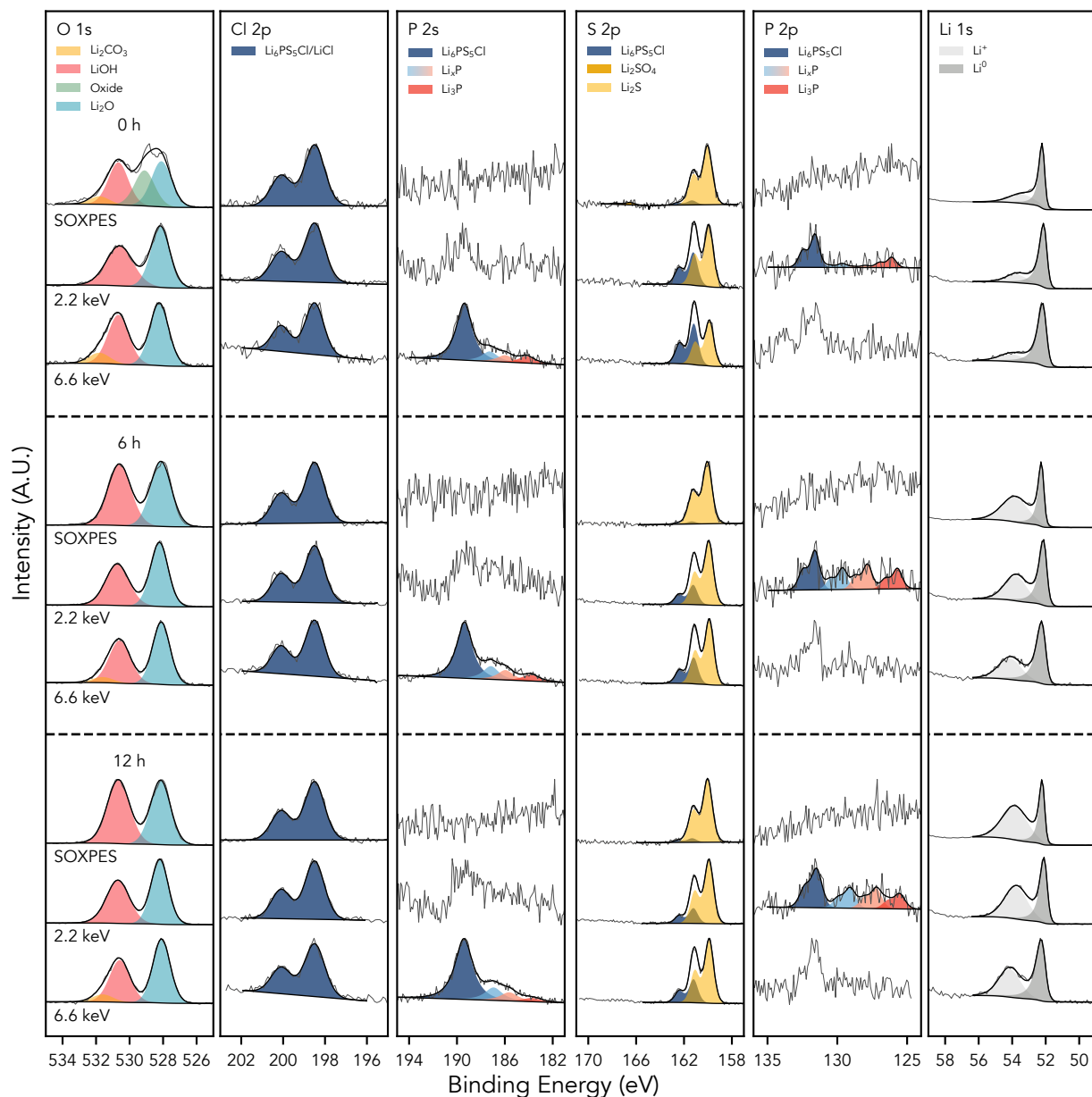


Figure S11: Full O 1s, Cl 2p, P 2s, S 2p, P 2p and Li 1s SOXPES and HAXPES spectra after approximately 20 nm of Li was evaporated onto a $\text{Li}_6\text{PS}_5\text{Cl}$ pellet. Photoelectrons emitted during SOXPES have a kinetic energy of 315 eV, and HAXPES was performed with incident photon energies of 2.2 and 6.6 keV. Measurements were performed 0, 6 and 12 h after Li evaporation. Source data are provided as a Source Data file.

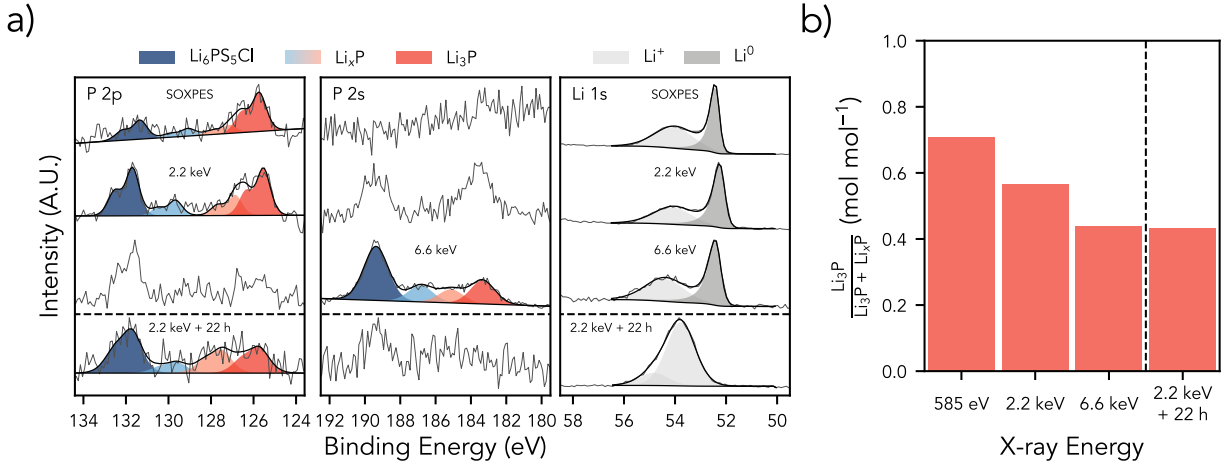


Figure S12: Soft and hard X-ray photoelectron spectroscopy (SOXPES and HAXPES) on an $\text{Li}_6\text{PS}_5\text{Cl}$ pellet with ~ 20 nm of Li evaporated on top. a) P 2p, P 2s and Li 1s spectra gathered using SOXPES (photon energies of 585, 645 and 505 eV for the P 2p, P 2s and Li 1s regions, respectively) and HAXPES with photon energies of 2.2 and 6.6 keV. HAXPES with 2.2 keV photons was additionally performed following a 22 h waiting period where all Li^0 had reacted, as evident from the disappearance of the Li^0 peak. The P 2p spectra display the best signal-to-noise ratio for the SOXPES and 2.2 keV HAXPES data, while the P 2s spectrum is best for the 6.6 keV HAXPES data as the photoionization cross section of the P 2s orbital exceeds that of the P 2p orbital at high incident photon energies [6]. These spectra were therefore used for subsequent analysis, as denoted by the fitted peaks. b) mole fraction of Li_3P in the P-containing SEI species calculated from the spectra in a), demonstrating a reduction in proportion of Li_3P with increasing probing depth and increasing time. Source data are provided as a Source Data file.

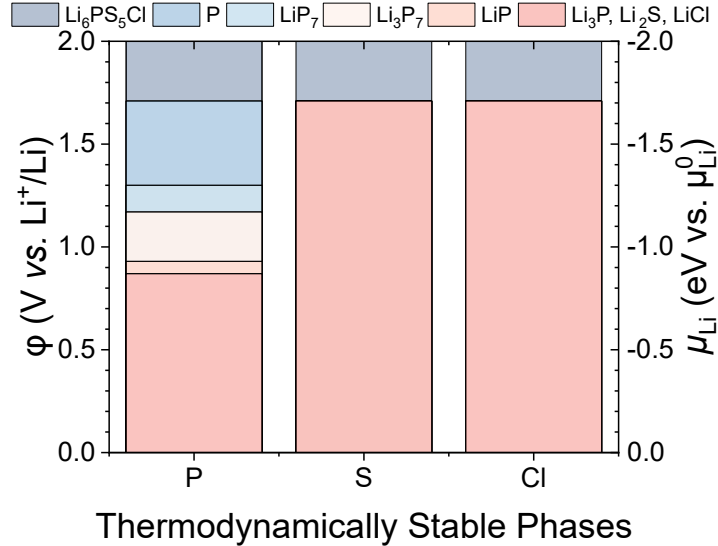


Figure S13: Thermodynamic stabilities of the elemental components of $\text{Li}_6\text{PS}_5\text{Cl}$ in the reductive region,[1].

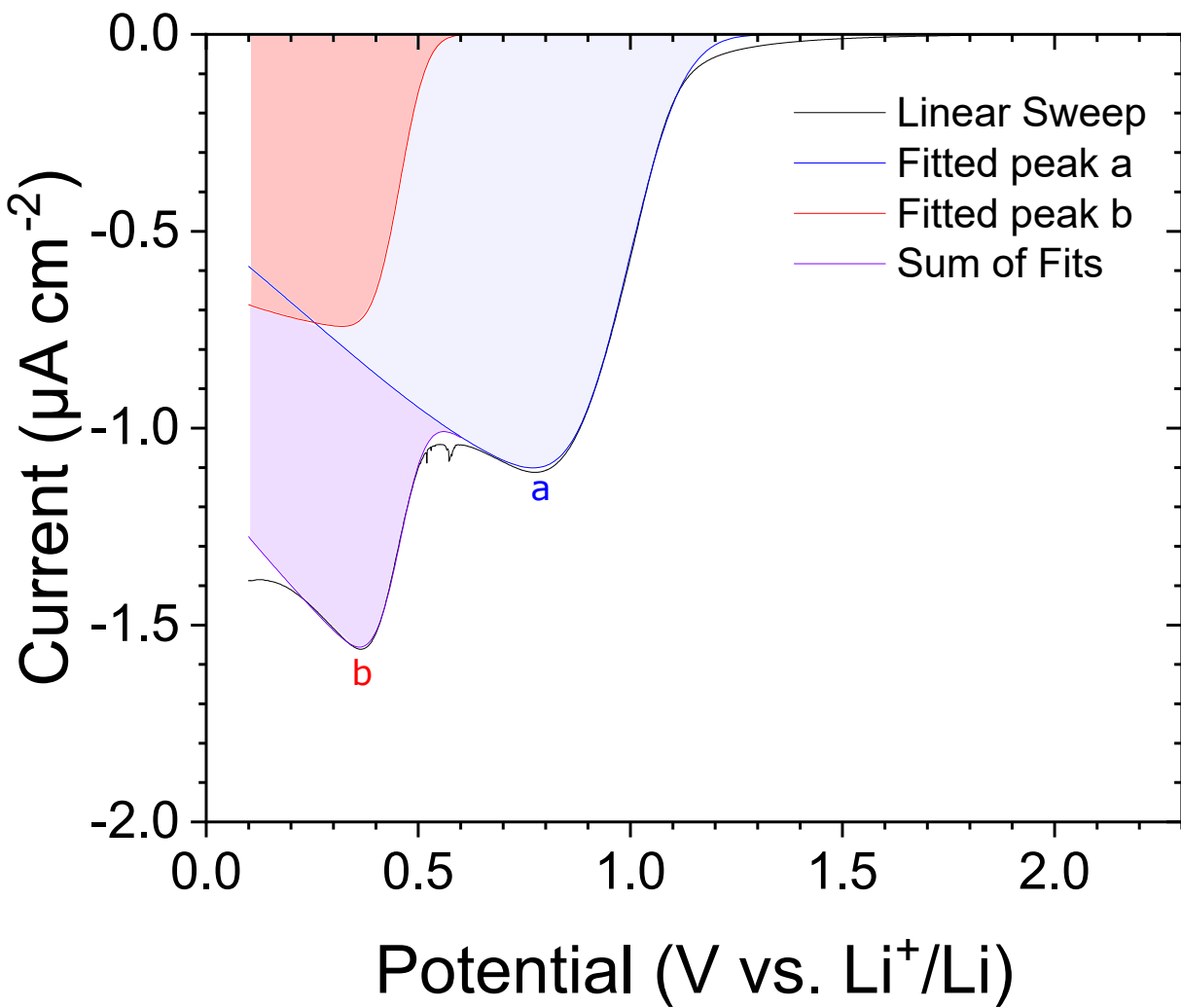


Figure S14: The initial linear sweep of the cyclic voltammetry, with peaks fitted to skewed Gaussians. The area under peak a corresponds to $2.36 \mu\text{Ah cm}^{-2}$, whilst the area under peak b corresponds to $0.72 \mu\text{Ah cm}^{-2}$. The total capacity of $3.08 \mu\text{Ah cm}^{-2}$ would correspond to an SEI thickness of 28 nm, if it was fully dense and consisted of Li_2S , LiCl and Li_3P . Source data are provided as a Source Data file.

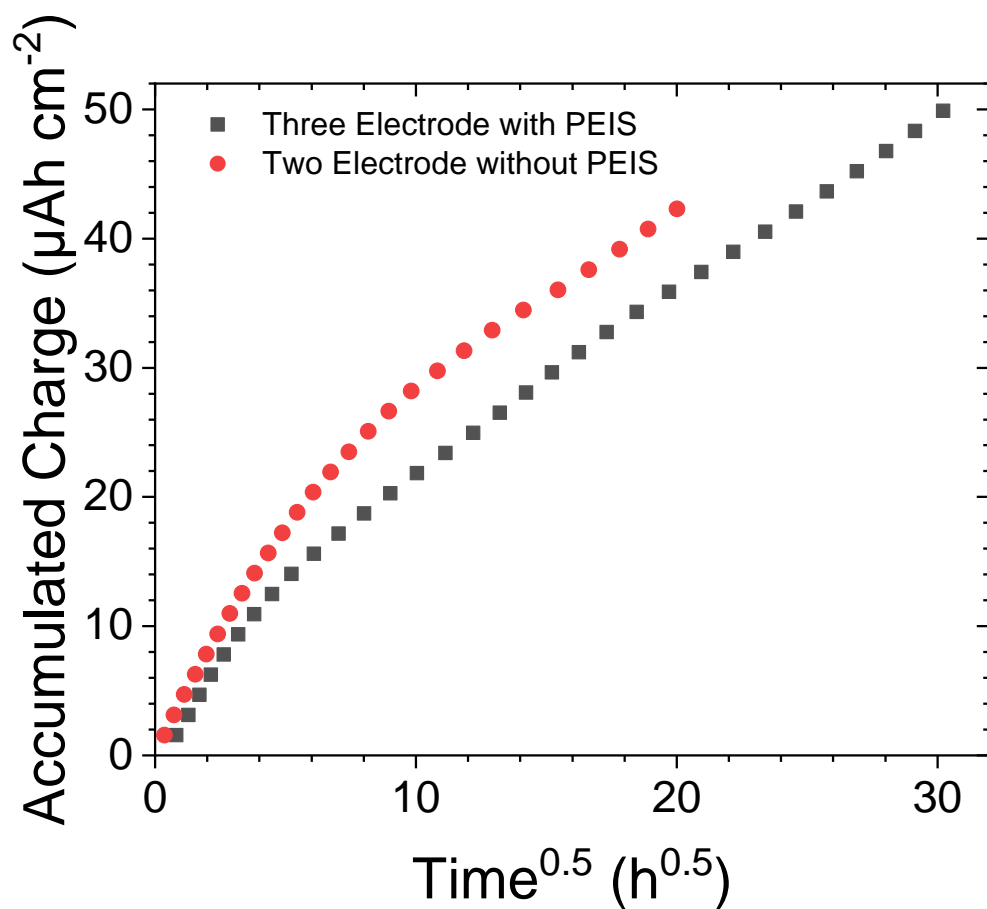


Figure S15: A comparison between three electrode and two electrode CTTA measurements. The three electrode cell conducted PEIS once a 50 mV OCV was reached before applying more reducing current, whilst the two electrode cell did not conduct PEIS and applied more reducing current as soon as 50 mV OCV was reached. Each plating step was $-1.56 \mu\text{A cm}^{-2}$ for 10 minutes. The cell pressure was 13 MPa and the temperature 303 K. Source data are provided as a Source Data file.

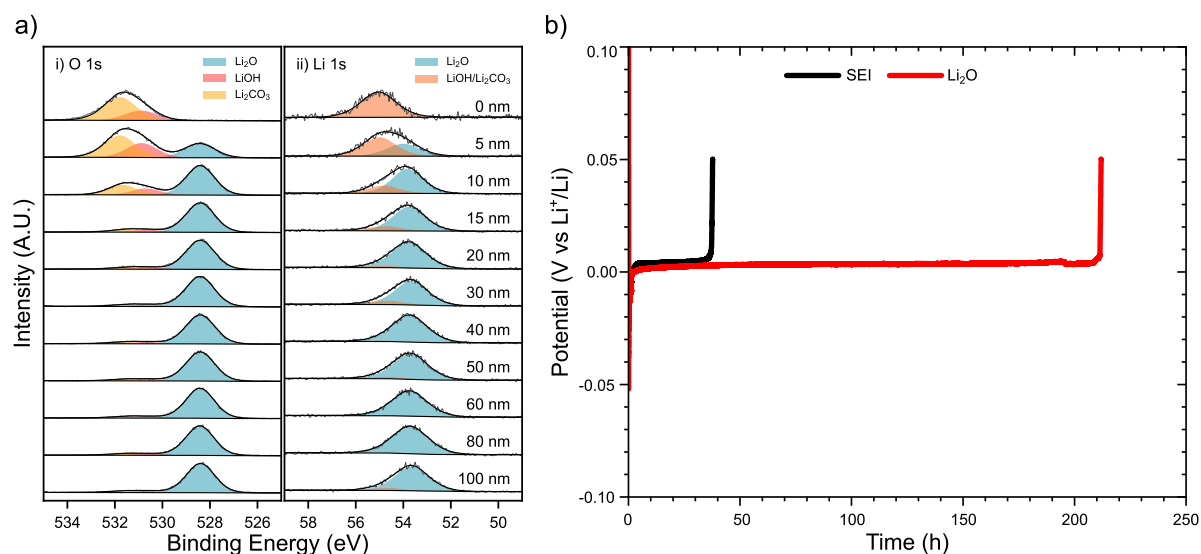


Figure S16: Rate of SEI formation through a preexisting SEI and a native passivation layer. a) Depth profiling of a 100 nm layer of thermally evaporated Li left in an Ar glovebox for two weeks (i, oxygen spectra; ii, Li spectra) revealing that except for a surface carbonate the entire film has turned into an oxide, b) the time taken for 0.02 mAh cm^{-2} (~ 100 nm) of electroplated Li to react through SEI formed from 0.02 mAh cm^{-2} (~ 100 nm) of Li reacting with $\text{Li}_6\text{PS}_5\text{Cl}$ (black) and Li_2O formed from allowing a 100 nm layer of thermally evaporated Li to react naturally in a Ar glovebox (< 0.01 ppm of O_2 and H_2O) for 2 weeks (red). Source data are provided as a Source Data file.

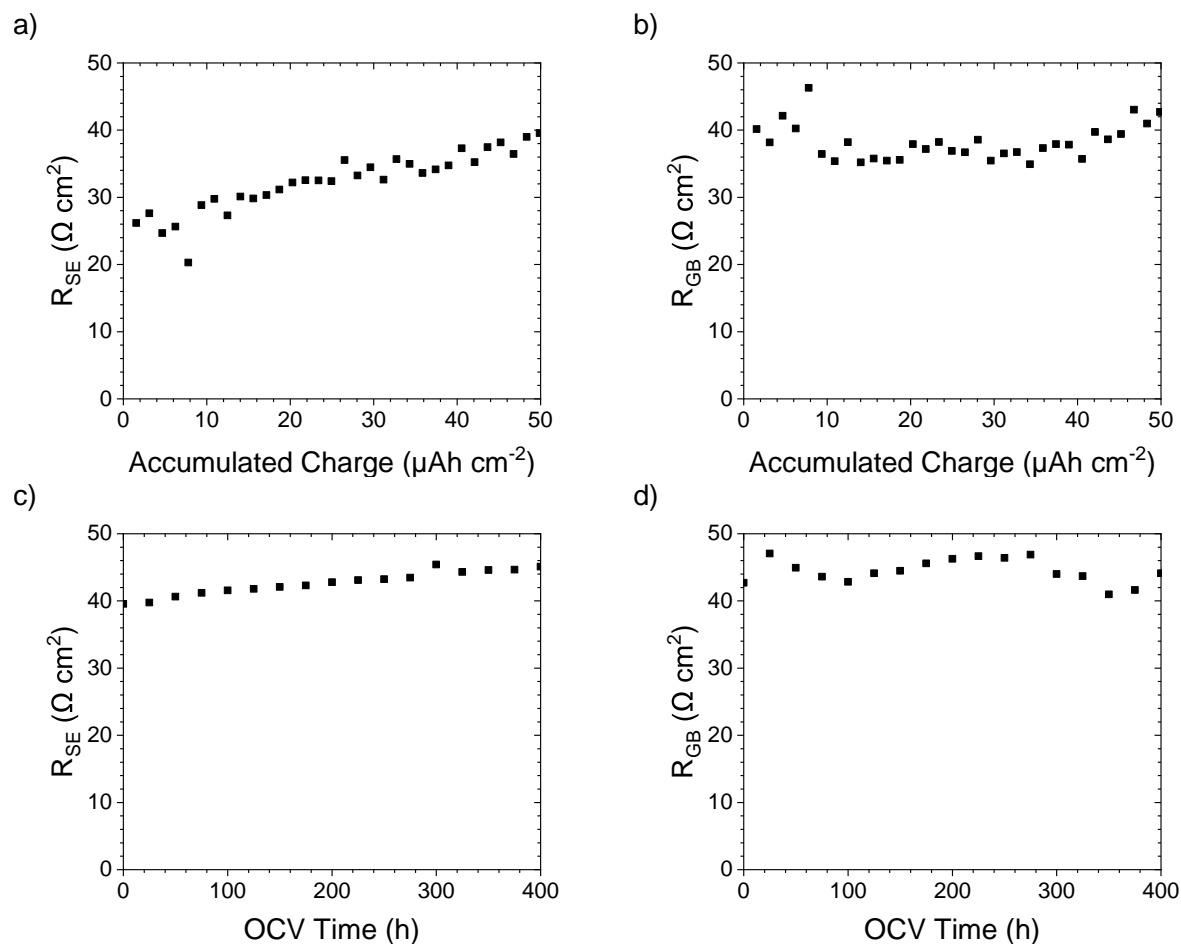


Figure S17: Bulk solid electrolyte (a,c) and grain boundary (b,d) resistance values obtained from fits of the impedance data shown in Figure 2c (a,b) and Figure 3a (c,d). The bulk solid electrolyte resistance (R_{SE}) is seen to slightly increase over the course of the measurement, which could be due to a slight degradation of the solid electrolyte over time through reaction with the reference electrode. Source data are provided as a Source Data file.

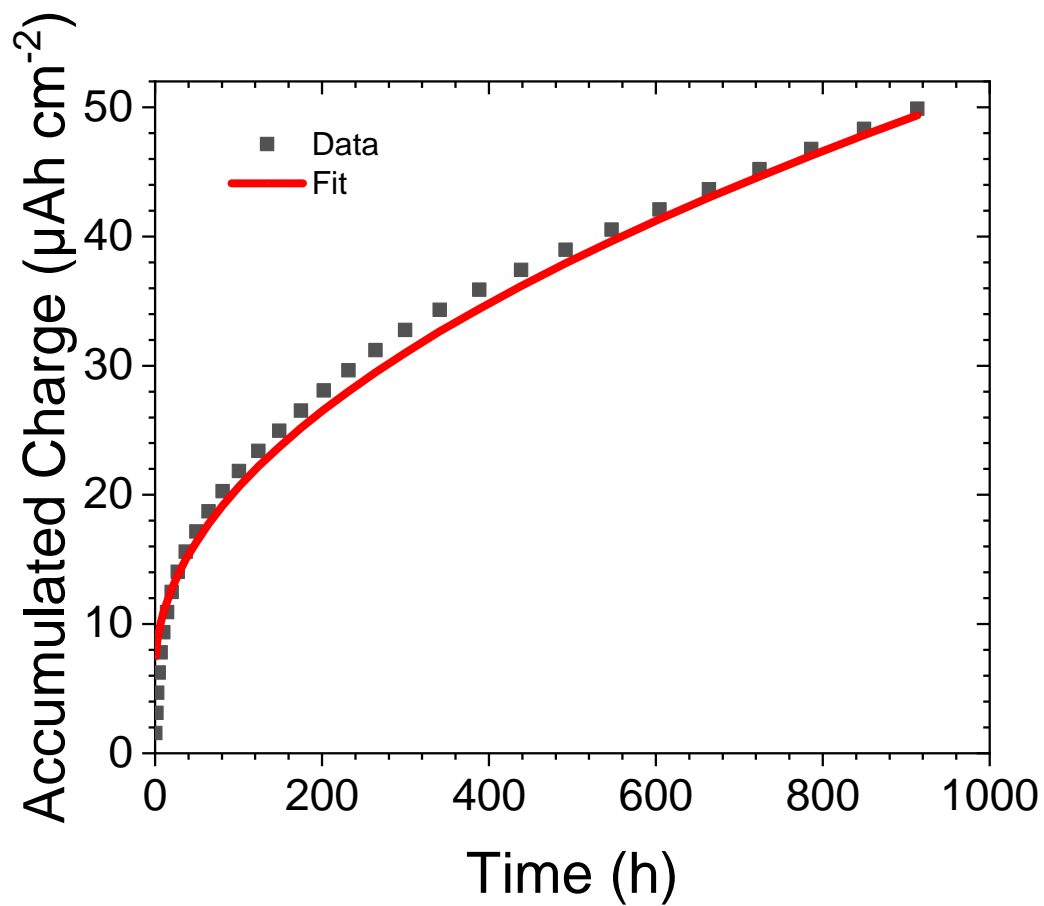


Figure S18: Fitting the CTTA data from Figure 1b to the Deal-Grove model,[2] with a fixed B of 2.025 (deduced from the fit line in Figure 1b) and allowing an A and τ to be deduced that optimise the fit. A was found to be -12.724, whilst τ was -19.988.

References

1. Zhu, Y., He, X. & Mo, Y. Origin of Outstanding Stability in the Lithium Solid Electrolyte Materials: Insights from Thermodynamic Analyses Based on First-Principles Calculations. *ACS Applied Materials and Interfaces* **7**, 23685–23693 (2015).
2. Deal, B. E. & Grove, A. S. General Relationship for the Thermal Oxidation of Silicon. *Journal of Applied Physics* **36**, 3770–3778 (1965).
3. BioLogic. *How to fit transmission lines with ZFit (EIS transmission lines) Battery – Application Note 43*
4. Capone, I. *et al.* Electrochemo-Mechanical Properties of Red Phosphorus Anodes in Lithium, Sodium, and Potassium Ion Batteries. *Matter* **3**, 2012–2028 (2020).
5. Tanuma, S., Powell, C. J. & Penn, D. R. Calculations of electron inelastic mean free paths. IX. Data for 41 elemental solids over the 50 eV to 30 keV range. *Surf. Interface Anal.* **43**, 689–713 (2011).
6. Yeh, J. J. & Lindau, I. Atomic subshell photoionization cross sections and asymmetry parameters: $1 \leq Z \leq 103$. *At. Data Nucl. Data Tables* **32**, 1–155 (1985).